A general derivation of the subharmonic threshold for non-linear bubble oscillations

Andrea Prosperetti[a)]
Department of Mechanical Engineering, Johns Hopkins University, Baltimore, Maryland 21218

(Received 31 August 2012; accepted 1 April 2013)

The paper describes an approximate but rather general derivation of the acoustic threshold for a subharmonic component to be possible in the sound scattered by an insonified gas bubble. The general result is illustrated with several specific models for the mechanical behavior of the surface coating of bubbles used as acoustic contrast agents. The approximate results are found to be in satisfactory agreement with fully non-linear numerical results in the literature. The amplitude of the first harmonic is also found by the same method. A fundamental feature identified by the analysis is that the subharmonic threshold can be considerably lowered with respect to that of an uncoated free bubble if the mechanical response of the coating varies rapidly in the neighborhood of certain specific values of the bubble radius, e.g., because of buckling.
 [http://dx.doi.org/10.1121/1.4802742]

PACS number(s): 43.25.Yw, 43.25.Ba, 43.80.Qf [SWY] Pages: 3719–3726

I. INTRODUCTION

Research on the use of contrast agents to enhance ultrasonic imaging of living tissue has recently focused on the use of the subharmonic component of the scattered sound (see, e.g., Shankar *et al.*, 1999; Chomas *et al.*, 2002; Goertz *et al.*, 2007; Frinking *et al.*, 2010; Faez *et al.*, 2011). The main advantage offered by this frequency band in comparison with the fundamental and its harmonics lies in the essential feature that, while the latter can be due to tissue as well as to contrast agents, there are virtually no subharmonic sources other than the contrast agents themselves. This feature obviates the need for the complex data-processing and filtering procedures made necessary by reliance on other frequency bands (see, e.g., Shankar *et al.*, 1998; Burns *et al.*, 2000).

Ultrasonic contrast agents are essentially gas bubbles stabilized against dissolution in the tissues by coatings of various nature. Thus, interest in the subharmonic emission is motivated by considerations very similar to those proposed in the past to monitor the occurrence of acoustic cavitation activity, which also requires unequivocal bubble-related acoustic signals in otherwise silent frequency bands (see, e.g., De Santis *et al.*, 1967; Eller and Flynn, 1969; Neppiras, 1969a,b; Neppiras and Coakley, 1976).

Unlike harmonics, which gradually set in as the excitation amplitude is increased, the subharmonic emission requires that a certain threshold be exceeded. A satisfactory theory for this threshold for the case of uncoated gas bubbles has been available for some time (Prosperetti, 1974, 1977). What motivates a reconsideration of this matter is the coating used to stabilize the bubbles, which has a major effect on the threshold. For this reason, several recent papers have presented numerical simulations and extensions of the somewhat involved classical theory to various specific models of the coating rheology (Sijl *et al.*, 2010; Katiyar and Sarkar, 2011).

The purpose of the present paper is to treat the problem perturbatively but with some degree of generality avoiding the adoption of specific models for the coating rheology (Sec. III). The effect of various modeling choices can then be checked directly on the final result (Sec. VI) as we show with several examples (Sec. VIII). The derivation is based on a simple heuristic argument (Sec. V) developed in an earlier paper (Prosperetti, 1976). By the same method, we also obtain an expression for the dependence of the first-harmonic scattering on the amplitude of the ultrasonic excitation (Sec. X).

Even though our results only hold in the small-amplitude approximation, it may be expected that their dependence on the various parameters reflects the trends of the actual phenomenon. In particular, it is shown that the presence of special values of the bubble radius in correspondence of which the rheology of the coating exhibits a rapid transition, e.g., due to buckling, considerably lowers the subharmonic threshold.

II. RADIAL DYNAMICS OF A COATED BUBBLE

Our starting point is a modified form of the Rayleigh–Plesset equation governing the radial dynamics of a spherical bubble of radius $R(t)$ (see, e.g., Brenner *et al.*, 2002):

$$R\ddot{R}+\frac{3}{2}\dot{R}^2=\frac{1}{\rho}\left[\left(1+\frac{R}{c}\frac{d}{dt}\right)P(R,\dot{R})-p_\infty+p_A\cos\omega t-\Sigma(R,\dot{R})\right]-4\nu\frac{\dot{R}}{R}. \quad (1)$$

Here dots denote time differentiation, ρ, c, and ν are the liquid density, speed of sound, and kinematic viscosity, p_∞ the undisturbed ambient pressure and p_A the amplitude of the insonifying signal with angular frequency ω. The bubble internal pressure $P(R,\dot{R})$ has been assumed to depend on the bubble radius and its time derivative to allow for dissipative processes such as heat exchange with the liquid

a)Author to whom correspondence should be addressed. Also at: Physics of Fluids Group, Faculty of Science and Technology, and Burgers Centrum, University of Twente, 7500AE Enschede, Netherlands. Electronic mail: prosperetti@jhu.edu

(Prosperetti, 1991); an example of this dependency is given in Eq. (45) below. Similarly, the interfacial term has been written as $\Sigma(R,\dot{R})$ to allow for surface tension and the elastic and dissipative properties of the coating. For an uncoated bubble with the internal pressure treated according to the usual polytropic approximation one would have

$$P(R,\dot{R}) = P_0\left(\frac{R_0}{R}\right)^{3\kappa}, \quad \Sigma(R,\dot{R}) = \frac{2\sigma}{R}, \tag{2}$$

with R_0 the equilibrium radius of the bubble, P_0 the bubble internal pressure when $R = R_0$ and σ the surface tension coefficient. The application of the general theory to several different models for Σ is shown later.

For the following developments, it is useful to set

$$\frac{R(t)}{R_0} = 1 + X(t), \tag{3}$$

with which the radial equation becomes

$$\ddot{X} + \frac{3}{2}\frac{\dot{X}^2}{1+X} = \frac{1}{\rho R_0^2(1+X)}[P(X,\dot{X}) - p_\infty + p_A\cos\omega t - \Sigma(X,\dot{X})] - \frac{4\nu}{R_0^2}\frac{\dot{X}}{(1+X)^2} + \frac{1}{\rho c R_0}\frac{dP}{dt}. \tag{4}$$

III. SMALL-AMPLITUDE APPROXIMATION

We use a perturbative approach based on a Taylor series expansion and set

$$P(R,\dot{R}) \simeq P_0 + P_X X + P_{\dot{X}}\dot{X} + \frac{1}{2}P_{XX}X^2 + \frac{1}{2}P_{\dot{X}\dot{X}}\dot{X}^2 + P_{X\dot{X}}X\dot{X} + \cdots, \tag{5}$$

where $P_0 = P(R_0, 0)$ and subscripts denote differentiation, and, similarly,

$$\Sigma(R,\dot{R}) = \Sigma_0 + \Sigma_X X + \Sigma_{\dot{X}}\dot{X} + \frac{1}{2}\Sigma_{XX}X^2 + \frac{1}{2}\Sigma_{\dot{X}\dot{X}}\dot{X}^2 + \Sigma_{X\dot{X}}X\dot{X} + \cdots, \tag{6}$$

where $\Sigma_0 = \Sigma(R_0, 0)$. For example, for the standard uncoated free-bubble model (2), we have

$$P_X = -3\kappa P_0, \quad P_{XX} = 3\kappa(3\kappa+1)P_0, \tag{7}$$

$$\Sigma_X = -\frac{2\sigma}{R_0}, \quad \Sigma_{XX} = \frac{4\sigma}{R_0}, \tag{8}$$

with all the other derivatives vanishing. After substitution of these expansions into (4), with allowance for the equilibrium relation

$$P_0 - p_\infty - \Sigma_0 = 0, \tag{9}$$

and systematic truncation to second order, we find an equation which may be written as

$$\ddot{X} + 2b\dot{X} + \omega_0^2 X = 2P_A\cos\omega t + AX^2 + B\dot{X}^2 + CX\dot{X} - 2P_A X\cos\omega t, \tag{10}$$

in which we have introduced the following definitions:

$$P_A = \frac{p_A}{2\rho R_0^2}, \tag{11}$$

$$\omega_0^2 = \frac{-P_X + \Sigma_X}{\rho R_0^2}, \quad 2b = 4\frac{\nu}{R_0^2} - \frac{P_X}{\rho c R_0} - \frac{P_{\dot{X}} - \Sigma_{\dot{X}}}{\rho R_0^2}, \tag{12}$$

$$A = \frac{1}{\rho R_0^2}\left[\frac{1}{2}(P_{XX} - \Sigma_{XX}) - (P_X - \Sigma_X)\right] = \frac{1}{2\rho R_0^2}(P_{XX} - \Sigma_{XX}) + \omega_0^2, \tag{13}$$

$$B = \frac{P_{\dot{X}\dot{X}} - \Sigma_{\dot{X}\dot{X}}}{2\rho R_0^2} - \frac{3}{2}, \tag{14}$$

$$C = \frac{P_{X\dot{X}} - \Sigma_{X\dot{X}} - P_{\dot{X}} + \Sigma_{\dot{X}}}{\rho R_0^2} + \frac{8\nu}{R_0^2}. \tag{15}$$

In deriving these expressions, we have approximated the term dP/dt as $P_X\dot{X}$, which is permissible in view of the large numerical value of the speed of sound in the liquid.

The quantity ω_0 has the physical meaning of the natural angular frequency of the linear model and from (7) and (8), for an uncoated bubble, it has the familiar expression

$$\omega_0^2 = \frac{1}{\rho R_0^2}\left(3\kappa P_0 - \frac{2\sigma}{R_0}\right). \tag{16}$$

Damping is described by the parameter b in the definition (12) of which we recognize, in order, the contributions due to the liquid viscosity, acoustic radiation, heat exchange with the liquid and surface viscosity.

IV. LINEAR THEORY

We denote by X_l the solution of the linear truncation of (10):

$$\ddot{X}_l + 2b\dot{X}_l + \omega_0^2 X_l = 2P_A\cos\omega t. \tag{17}$$

At steady state, X_l is given by

$$X_l = X_0 e^{i\omega t} + \text{c.c.} \quad \text{with} \quad X_0 = \frac{P_A}{\omega_0^2 - \omega^2 + 2ib\omega}, \tag{18}$$

where, here and in the following, c.c. denotes the complex conjugate. If ω is very different from ω_0 and P_A is small, X_l will also be small. However, if $\omega \sim \omega_0$ and the damping is small, X_l becomes substantial even with a weak forcing.

This mechanism of resonant amplification is at the root of the frequency spectrum of a non-linear oscillator as will be seen in the next section.

V. NON-LINEAR RESONANCES

We now set, in (10),

$$X(t) = X_l(t) + Y(t), \tag{19}$$

with $X_l(t)$ given by (18), and find

$$\ddot{Y} + 2b\dot{Y} + \omega_0^2 Y = A(X_l + Y)^2 + B(\dot{X}_l + \dot{Y})^2 + C(X_l + Y)(\dot{X}_l + \dot{Y}) - 2P_A(X_l + Y)\cos\omega t. \tag{20}$$

Although, of course, the Y in the right-hand side of this equation is the same as that in the left-hand side, it is useful to consider it for a moment as a given driving force. In this sense, the equation may be seen as describing the response of the linear oscillator in the left-hand side to the excitation provided by the right-hand side which, due to its non-linear nature, has a greater frequency content than that of the driving ultrasound.

Ordinarily, when the ultrasound amplitude is not large, the response Y will also be small and the additional frequencies will amount to only small features in the acoustic spectrum scattered by the bubble. This conclusion however must be modified when one of the frequencies in the right-hand side of (20) is close to ω_0 as, in this case, the linear oscillator in the left-hand side will contain a significant component at a frequency close to ω_0 by the resonant amplification mechanism mentioned at the end of the previous section.

It is easy to determine which are the possible insonifying frequencies that can determine a strong response in this way. As just explained, for these frequencies we expect Y to contain a significant component proportional to $e^{\pm i\nu\omega t}$, with $\nu\omega \sim \omega_0$. Thus, the "combination tones" due to the interaction of this dominant component of Y with X_l in the right-hand side of (20) will occur at frequencies

$$0, \quad 2\omega, \quad \omega \pm \nu\omega, \quad 2\nu\omega. \tag{21}$$

The only possible frequencies of this list which can resonate with the frequency $\omega_0 \sim \nu\omega$ of the left-hand side of (20) are $2\omega \sim \nu\omega$, i.e., $\nu = 2$, and $(1-\nu)\omega \sim \nu\omega$, i.e., $\nu = \frac{1}{2}$. In the first case the strong response will be at the first harmonic, in the second one at the first subharmonic. This is the essence of the argument originally presented in Prosperetti (1976). Superficially, this argument seems independent of ω_0 but, in reality, it is not as, unless $\nu\omega \sim \omega_0$, no resonant amplification is possible.

We conclude that, in order to find the dominant component of the solution of (20), it is sufficient to consider only the terms in the right-hand side which contain the resonant frequencies, as all the other terms will only give a small contribution to Y.

VI. SUBHARMONIC

On the basis of the previous argument, in the subharmonic frequency region, we write the dominant part of the solution of (20) as

$$Y \simeq Y_{1/2} = Y_0 e^{i\omega t/2} + \text{c.c.} \tag{22}$$

We substitute this approximation for Y into the right-hand side of (20) and, on the basis of the previous considerations, we discard all the terms which cannot give rise to combination tones close to ω_0. With this step, the equation becomes, approximately,

$$\ddot{Y}_{1/2} + 2b\dot{Y}_{1/2} + \omega_0^2 Y_{1/2} = \left[\left(2A + \omega^2 B + \frac{i}{2}\omega C\right)X_0 - P_A\right]\bar{Y}_0 e^{i\omega t/2} + \text{c.c.} \tag{23}$$

where the overline denotes the complex conjugate and X_0 is given in (18). The peculiarity of the subharmonic component lies in the fact that this equation can be satisfied by $Y_0 = 0$. This will be the only possible solution unless the right-hand side is able to supply enough energy to overcome the damping in the left-hand side. The origin of a threshold excitation for the subharmonic lies in the fact that, for this to happen, Y_0 itself must be sufficiently large, which imposes a condition on the amplitude of the drive.

After substitution of (22) into the left-hand side of (23), the terms proportional to $e^{i\omega t/2}$ will balance provided that

$$\left(\omega_0^2 - \frac{1}{4}\omega^2 + ib\omega\right)Y_0 - \left[\left(2A + \omega^2 B + \frac{i}{2}\omega C\right)X_0 - P_A\right]\bar{Y}_0 = 0. \tag{24}$$

Consideration of the terms proportional to $e^{-i\omega t/2}$ leads to the complex conjugate of this relation:

$$-\left[\left(2A + \omega^2 B - \frac{i}{2}\omega C\right)\bar{X}_0 - P_A\right]Y_0 + \left(\omega_0^2 - \frac{1}{4}\omega^2 - ib\omega\right)\bar{Y}_0 = 0. \tag{25}$$

These two relations form a homogeneous algebraic linear system for Y_0 and $\bar{Y}_0$ which can have nonzero solutions only provided the determinant vanishes. After some reduction, this condition may be written in the form

$$\left(\frac{P_A}{\sqrt{(\omega_0^2 - \omega^2)^2 + 4b^2\omega^2}}\right)^2 = \frac{\left(\omega_0^2 - \frac{1}{4}\omega^2\right)^2 + b^2\omega^2}{\left[2A + (B+1)\omega^2 - \omega_0^2\right]^2 + \left(\frac{1}{2}C - 2b\right)^2\omega^2}. \tag{26}$$

Since, unless this condition is satisfied, the only possible solution of (24) and (25) is $Y_0 = \bar{Y}_0 = 0$, it is evident that (26) determines the threshold for the subharmonic emission. The subharmonic amplitude remains undetermined in the present second-order theory, but can be found by carrying the theory to the third order as shown in an earlier paper (Prosperetti, 1974).

VII. ABSOLUTE THRESHOLD

The previous result (26) gives the threshold pressure amplitude for the subharmonic to be *possible*. In general, however, whether the subharmonic component is *actually*

excited or not, depends on the initial conditions of the motion. It is only when the subharmonic-free motion is unstable that the subharmonic is *necessarily present* (Prosperetti, 1974, 1977; Sijl *et al.*, 2010). For this to happen the pressure amplitude must exceed another threshold which may be termed the *absolute threshold*. An expression for this threshold cannot be derived truncating the small-amplitude expansion at second order as done in Sec. III. At least one more order is necessary. The relevant calculation can be found in Prosperetti (1974) and the final results are also given in Prosperetti (1977) and Sijl *et al.* (2010).[1]

The absolute threshold is mostly larger than the existence threshold except in the vicinity of $\omega/\omega_0 = 2$. An example for a 10 μm-radius bubble calculated with the parameter values of Fig. 5 of Prosperetti (1977) is shown in Fig. 1; here and in the following figures $f = \omega/2\pi$ and $f_0 = \omega_0/2\pi$.

The existence of two separate thresholds should be kept in mind when judging numerical results for which the distinction between them is not easily made.

VIII. EXAMPLES

We now apply the previous general result (26) to some specific coating rheology models used in the literature. Since the present theory is built on a weakly non-linear approximation, it is of particular interest to compare its predictions to the fully non-linear numerical results of Katiyar and Sarkar (2011).

In all the examples that follow, the bubble internal pressure P is modeled in the polytropic form (2) with $p_\infty = 101.3$ kPa, $\nu = 10^{-6}$ m^2/s and $\rho = 1000$ kg/m^3. The effect of the coating (or of surface tension for an uncoated bubble), is parameterized as

$$\Sigma = \frac{2\sigma(R)}{R} + 4\eta_s(R)\frac{\dot R}{R^2} = \frac{2\sigma}{R_0(1+X)} + 4\,\frac{\eta_s(X)\dot X}{R_0(1+X)^2}, \tag{27}$$

where η_s is the coefficient of surface viscosity.

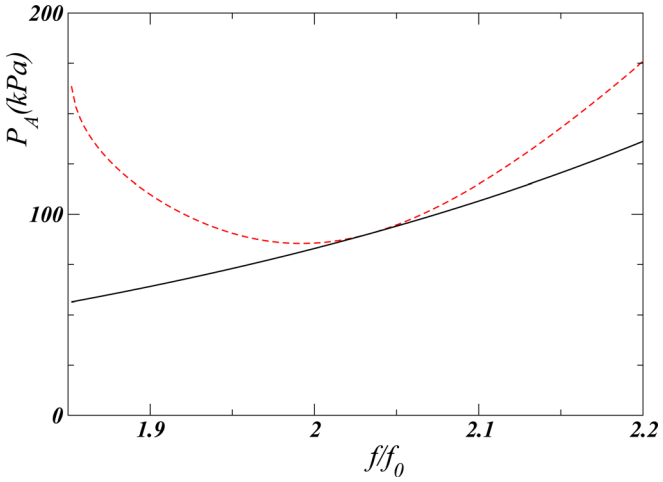

FIG. 1. (Color online) The solid line is the pressure amplitude above which a subharmonic component is *possible;* the dashed line is the pressure amplitude above which a subharmonic component is *necessarily present* due to the instability of the subharmonic-free oscillations. This example is for an uncoated free bubble with a 10 μm-radius using the parameter values of Fig. 5 of Prosperetti (1977).

A. Uncoated bubble

In the present notation, the subharmonic threshold of an uncoated bubble derived in Prosperetti (1977) and confirmed in Sijl *et al.* (2010) can be written as

$$\frac{P_A}{|\omega_0^2 - \omega^2|} = \frac{b\omega}{|2A - \frac{1}{2}\omega^2 - \omega_0^2|}. \tag{28}$$

In the theory leading to this result the damping parameter b was assumed to be very small, which explains its absence from the left-hand side where it is negligible compared to $\omega^2 - \omega_0^2 \sim \frac{3}{4}\omega^2$. Furthermore, in the derivation of (28), use was made of the simple model (2) so that $B = -\frac{3}{2}$ and $C = 4b$. Thus, if attention is limited to the neighborhood of $\omega \simeq \frac{1}{2}\omega$, it is seen that (26) is in excellent agreement with (28).

Katiyar and Sarkar (2011) have investigated this case numerically taking $c = 1485$ m/s, $\sigma = 0.072$ J/m^2, and $\kappa = 1.07$. Their results for a 3 μm-radius bubble (dashed line) are compared with the present one in Fig. 2. As expected, there are some differences, but the present approximation captures nevertheless the essential features of the threshold. An element to keep in mind in this comparison is that the numerical results really refer to what was termed the absolute threshold in Sec. VII. Therefore, the comparison becomes somewhat less meaningful away from $\omega/\omega_0 = 2$.

B. Viscous coating

For the simple model of a viscous coating one may use (27) with both the surface tension coefficient σ and the coefficient of surface viscosity η_s constants (Sarkar *et al.*, 2005). In this case

$$\Sigma_X = -\frac{2\sigma}{R_0}, \quad \Sigma_{\dot X} = \frac{4\eta_s}{R_0}, \quad \Sigma_{XX} = \frac{4\sigma}{R_0}, \quad \Sigma_{X\dot X} = -\frac{8\eta_s}{R_0}, \tag{29}$$

while the other derivatives of Σ vanish. Furthermore,

$$2b = 4\,\frac{\nu}{R_0^2} + \frac{4\eta_s}{\rho R_0^3} + \frac{3\kappa P_0}{\rho c R_0}, \quad C = \frac{4}{R_0^2}\left(2\nu + 3\,\frac{\eta_s}{\rho R_0}\right). \tag{30}$$

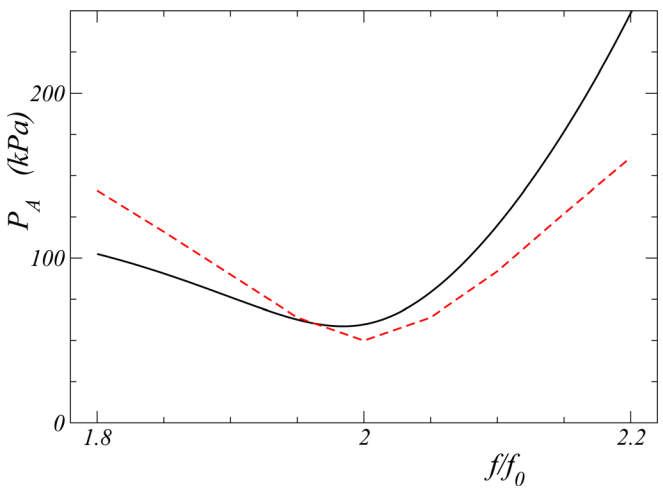

FIG. 2. (Color online) The present prediction for the subharmonic threshold for an uncoated free bubble with a radius of 3 μm (solid line) compared with the fully non-linear numerical results of Katiyar and Sarkar (2011) (dashed line).

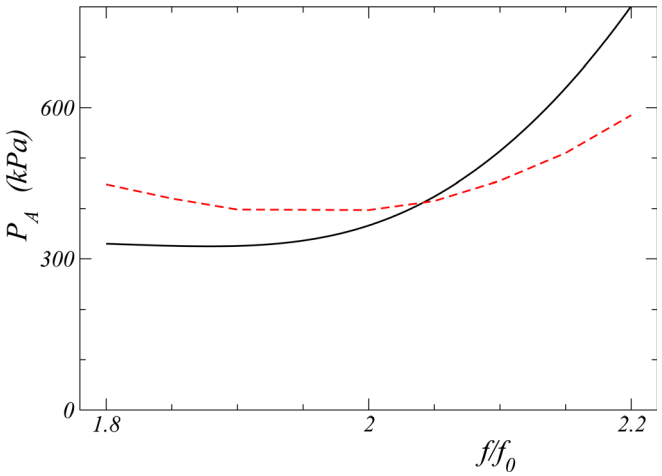

FIG. 3. (Color online) The present prediction for the subharmonic threshold for a 3 μm-radius bubble with a viscous coating (solid line) compared with the fully non-linear numerical results of Katiyar and Sarkar (2011) (dashed line).

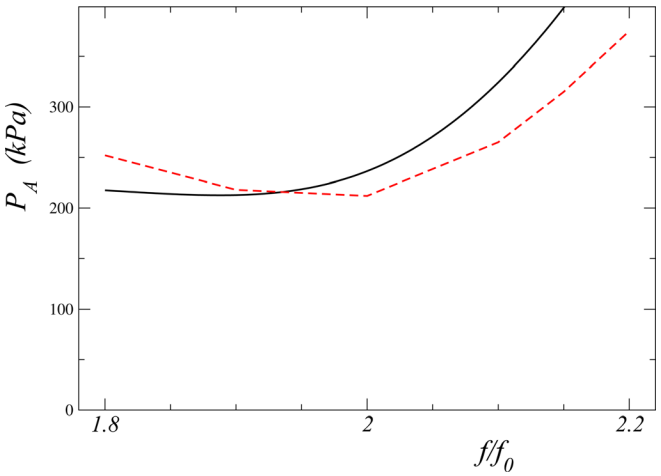

FIG. 4. (Color online) The present prediction for the subharmonic threshold for a Sonazoid bubble with a radius of 3 μm (solid line) compared with the fully non-linear numerical results of Katiyar and Sarkar (2011) (dashed line).

In order to compare with the numerical results of Katiyar and Sarkar (2011), we take $\sigma = 0.6$ J/m^2, $c = 1485$ m/s, $\kappa = 1.07$, and $\eta_s = 10^{-8}$ N s/m. The comparison is shown in Fig. 3 and is qualitatively similar to the uncoated-bubble case of the previous figure.

C. Church-Hoff model

The model proposed by Church (1995) and further developed by Hoff *et al.* (2000) can be cast in the form (27) by taking

$$\sigma(R) = 6G_s d_s \frac{R_0^2}{R^2}\left(1 - \frac{R_0}{R}\right), \quad \kappa(R) = 3\mu_s d_s \frac{R_0^2}{R^2}, \tag{31}$$

with which

$$\Sigma_X = \frac{12G_s d_s}{R_0}, \quad \Sigma_{\dot{X}} = \frac{12\mu_s d_s}{R_0}, \quad \Sigma_{\dot{X}\dot{X}} = 0, \tag{32}$$

$$\Sigma_{XX} = -\frac{96G_s d_s}{R_0}, \quad \Sigma_{X\dot{X}} = -\frac{48\mu_s d_s}{R_0}. \tag{33}$$

Katiyar and Sarkar (2011) have used this model to calculate the non-linear threshold for a 3 μm-radius Sonazoid bubble by taking $G_s = 52$ MPa, $\mu_s = 0.99$ Pa s, and $d_s = 4$ nm. Figure 4 shows a comparison of their results (dashed line) with the present ones. They have also adapted the same model to Levovist bubbles. The comparison of our to their result is similar to that of Fig. 4 and is not shown for brevity.

D. Model of Marmottant *et al.*

Marmottant *et al.* have introduced a model which accounts for the transition from an effectively vanishing surface tension, when the radius has shrunk so much that the coating buckles, to a surface tension equal to σ_0, the surface tension of an uncoated bubble, when the coating has ruptured (Marmottant *et al.*, 2005). The model may be written as

$$\sigma = \begin{cases} 0 & \text{for} \quad R \le R_b \\ \chi\left(\dfrac{R^2}{R_b^2} - 1\right) & \text{for} \quad R_b \le R \le R_{\text{rupture}} \\ \sigma_0 & \text{for} \quad R_{\text{rupture}} \le R, \end{cases} \tag{34}$$

with R_b the buckling radius, or, more compactly, as

$$\sigma(X) = \chi[H(X - X_b) - H(X - X_r)] + \sigma_0 H(X - X_r), \tag{35}$$

where H is the Heaviside step function, $X_b = R/R_b - 1$ and $X_r = R/R_{\text{rupture}} - 1$. In any real system the sharp transition modeled by the step function will be attenuated by the actual properties of the coating. It is therefore justified to use a smoothed approximation to the step function; a standard one is (see, e.g., Peskin, 1977; Engquist *et al.*, 2005; Towers, 2007)

$$H_\epsilon(x) = \frac{1}{2} + \frac{x + (\epsilon/\pi)\sin \pi x/\epsilon}{2\epsilon}, \tag{36}$$

from which

$$H'_\epsilon(x) = \delta_\epsilon(x) = \frac{1 + \cos \pi x/\epsilon}{2\epsilon},$$
$$\delta'_\in(x) = -\frac{\pi}{2\epsilon^2}\sin\ \pi x/\epsilon. \tag{37}$$

These functions reduce to $H(x)$, $\delta(x)$, and $\delta'(x)$, respectively, as $\varepsilon \to 0$.

With these expressions and a constant coefficient of surface viscosity, for $R_0 = R_b$, we find

$$\Sigma = 0, \quad \Sigma_X = 2\frac{\chi}{R_b}, \quad \Sigma_{XX} = 4\frac{\chi}{R_b}\left[\frac{1}{\epsilon} - \frac{1}{2}\right], \tag{38}$$

$$\Sigma_{\dot{X}} = \frac{4\kappa}{R_0}, \quad \Sigma_{X\dot{X}} = -\frac{8\kappa}{R_0}, \tag{39}$$

while $\Sigma_{\dot{X}\dot{X}} = 0$. To gain some insight into the behavior of this model, we can assume $\varepsilon \ll 1$ and evaluate the expression (26) at $\omega = 2\omega_0$; the result is

$$\frac{P_A}{\sqrt{9\omega_0^2 + 16b^2}} \simeq \left(\frac{3}{2}\kappa\frac{R_b P_0}{\chi} + 1\right) b\epsilon. \tag{40}$$

The threshold can be made as small as desired by decreasing ε.

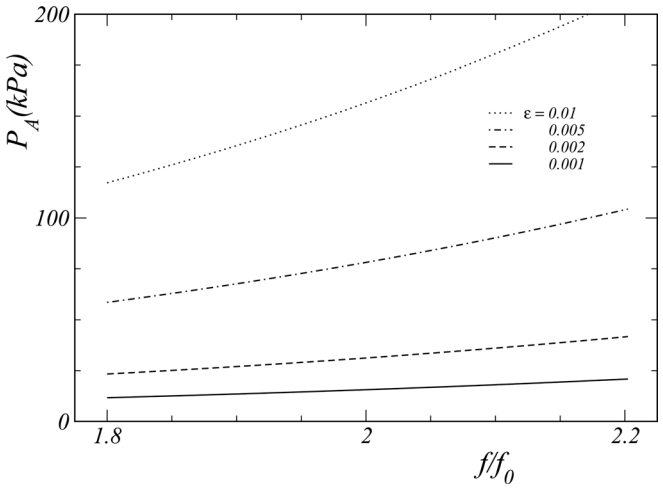

FIG. 5. Subharmonic threshold according to the model of Marmottant *et al.* (2005). The different lines correspond to different values of the regularization parameter ε; see Sec. VIII D for details. Note how strongly the threshold can be reduced with respect to the case of an uncoated bubble shown in Fig. 2.

For a numerical example, following Marmottant *et al.* (2005), we take $\rho = 1000$ kg/m^3, $\nu = 10^{-6}$ m^2/s, $c = 1480$ m/s, $\chi = 1$ N/m, $\eta_s = 15 \times 10^{-9}$ N, $R_b = 0.975$ μm, $\kappa = 1.095$ and vary ε. Figure 5 shows the predicted thresholds for the existence of the subharmonic for $10^{-3} \le \varepsilon \le 10^{-2}$.

A different regularization of the previous model has recently been proposed by Sijl *et al.* (2010) who write

$$\sigma(X) = \sigma_0 + 2\hat{\chi}X + \frac{1}{2}\zeta X^2. \tag{41}$$

If R_0 corresponds to the buckling radius, $\sigma_0 = 0$ and $\zeta > 0$. For R_0 in the neighborhood of the rupture radius, on the other hand, $\sigma_0 = 0.072$ J/m^2 and $\zeta < 0$. With this expression, we find

$$\Sigma_X = 2\frac{2\hat{\chi} - \sigma_0}{R_0}, \quad \Sigma_{XX} = 2\frac{\zeta - 4\hat{\chi} + 2\sigma_0}{R_0}, \tag{42}$$

while the other derivatives are the same as in (39). A comparison of the expression for Σ_{XX} with that shown in (39) shows that, approximately, the role played by $4\chi/\varepsilon$ in (39) is the same as that of $2(\zeta - 4\hat{\chi})$ in (42) and, indeed, Sijl *et al.* (2010) show that the subharmonic threshold greatly decreases by increasing $\zeta - 4\hat{\chi}$ similarly to what is shown in Fig. 5.

IX. MINIMIZING THE SUBHARMONIC THRESHOLD

Let us now consider in general terms how the subharmonic threshold can be reduced. Since the minimum of the threshold occurs in the neighborhood of $\omega_0 = \frac{1}{2}\omega$, let us rewrite the general expression (26) for $\omega = 2\omega_0$; we find

$$\left(\frac{P_A}{\omega_0\sqrt{9\omega_0^2+16b^2}}\right)^2 = \frac{4b^2}{[2A/\omega_0^2+4B+3]^2+4\left(\frac{1}{2}C-2b\right)^2}. \tag{43}$$

From their definitions, we see that

$$2\frac{A}{\omega_0^2} + 4B + 3 = -\frac{d}{dX}\log(-P_X + \Sigma_X) - 1 + \frac{P_{\dot{X}\dot{X}} + \Sigma_{\dot{X}\dot{X}}}{2\rho R_0^2}. \tag{44}$$

The bubble internal pressure depends on the bubble radius, frequency, and nature of the gas, but for the small bubbles of present concern, it will be close to isothermal. Thus, the pressure terms in this relation cannot be easily manipulated. The effect of the radial velocity is approximately embodied in the relation (Prosperetti, 1991)

$$\frac{P}{P_0} = \left(\frac{R_0}{R}\right)^3\left(1 - \frac{\gamma - 1}{5\gamma}\frac{R_0^3}{DR^2}\dot{R}\right) = (1+X)^{-3} - \frac{\gamma - 1}{5\gamma}\frac{R_0^2}{D}(1+X)^{-5}\dot{X}, \tag{45}$$

with γ the ratio of the specific heats and D the thermal diffusivity of the gas, from which it is seen that $P_{\dot{X}\dot{X}} = 0$. For models of the type (27), $\Sigma_{\dot{X}\dot{X}} = 0$. The most effective way to decrease the threshold by increasing (44) appears therefore to endow the coating with a large value of $(d/dX)\log\Sigma_X = \Sigma_{XX}/\Sigma_X$. In the model of Marmottant *et al.* (2005), for $R_0 = R_b$, $\Sigma_{XX}/\Sigma_X = (2-\varepsilon)/\varepsilon$, which reflects the near-discontinuity of Σ_X in the neighborhood of the buckling radius. It would appear that any coating the properties of which change rapidly for particular values of the radius (e.g., due to the transition to a close-packing of the constituent molecules) would endow bubbles having a similar radius with a very low subharmonic threshold.

Another way to decrease the threshold would be to increase the combination $\frac{1}{2}C - 2b$ without increasing the damping b. From the definitions (12) and (15), with the models (45) for the pressure and (27) for the surface properties, we find

$$\frac{1}{2}C - 2b = \frac{2}{5}\frac{\gamma - 1}{\gamma}\frac{P_0}{\rho D} - \frac{3\kappa P_0}{\rho c R_0} + 2\frac{\eta_s - d\eta_s/dX}{\rho R_0^3}. \tag{46}$$

The first term also occurs in the expression for b, which is

$$2b = 4\frac{\nu}{R_0^2} + \frac{\gamma - 1}{5\gamma}\frac{P_0}{\rho D} + \frac{3\kappa P_0}{\rho c R_0} + \frac{4\eta_s}{\rho R_0^3}, \tag{47}$$

and, therefore, cannot be increased independently from b. The second term (acoustic damping) is quantitatively of minor importance. The most effective way to increase $\frac{1}{2}C - 2b$ seems therefore to be to make $d\eta_s/dX$ more and more negative while, at the same time, limiting the increase of η_s. Hence, again, we see the benefit of the rapid variation of a coating property—the surface viscosity η_s rather than the surface elasticity as before—near particular values of the radius.

X. HARMONIC

A treatment of the first harmonic response can be provided along lines similar to those used in Sec. VI. In this case we set, in place of (22),

$$Y \simeq Y_2 = Y_0 e^{2i\omega t} + \text{c.c.}, \tag{48}$$

and, retaining only resonant terms, approximate (20) by

$$\ddot{Y}_2 + 2b\dot{Y}_2 + \omega_0^2 Y_2 = [AX_0^2 - \omega^2 BX_0^2 + i\omega CX_0^2 - P_A X_0] e^{2i\omega t} + \text{c.c.} \tag{49}$$

It is obvious that $Y_0 = 0$ is not a solution of this equation. Thus, the harmonic component does not exhibit a threshold: whatever the driving, a nonzero harmonic component is necessarily present.

After substitution of (48) in the left-hand side of (49) and some rearrangement one finds

$$|Y_0|^2 = \left(\frac{P_A}{\sqrt{(\omega_0^2 - \omega^2)^2 + 4b^2\omega^2}} \right)^4 \times \frac{[A + (1-B)\omega^2 - \omega_0^2]^2 + (C+2b)^2\omega^2}{(\omega_0^2 - 4\omega^2)^2 + 16b^2\omega^2}. \tag{50}$$

For an uncoated bubble this becomes

$$|Y_0|^2 = \left(\frac{P_A}{\sqrt{(\omega_0^2 - \omega^2)^2 + 4b^2\omega^2}} \right)^4 \times \frac{\left[A + \frac{5}{2}\omega^2 - \omega_0^2\right]^2 + 36b^2\omega^2}{(\omega_0^2 - 4\omega^2)^2 + 16b^2\omega^2}, \tag{51}$$

which can be compared with the earlier expression (Prosperetti, 1974):

$$|Y_0|^2 = \left(\frac{P_A}{\omega_0^2 - \omega^2} \right)^4 \frac{\left[A + \frac{5}{2}\omega^2 - \omega_0^2\right]^2}{(4\omega^2 - \omega_0^2)^2 + 16b^2\omega^2}. \tag{52}$$

As in the previous case, the two results coincide except for the small terms $4b^2$ and $36b^2$, which are both negligible. Of course, the term $16b^2$ in the right-hand side denominator cannot be dropped as this result is to be used in the neighborhood of $2\omega \sim \omega_0$.

It may be noted that attempts to increase the quantity A in order to lower the subharmonic threshold would in most cases also have the effect of increasing the scattering amplitude of the first harmonic.

XI. SUMMARY AND CONCLUSIONS

We have provided a simple derivation of the smallest acoustic pressure amplitude necessary for the presence of a steady subharmonic component in the ultrasound scattered by a spherical bubble. By virtue of its generality, the result can be readily adapted to a variety of models for the surface coating of bubbles used as acoustic contrast agents, and we have provided several examples in Sec. VIII.

A fundamental feature identified by the analysis is that the subharmonic threshold can be considerably lowered with respect to that of an uncoated bubble if the mechanical response of the coating varies rapidly in the neighborhood of certain specific values of the bubble radius, e.g., because of buckling (or, possibly, rupture). The reason is that the subharmonic response is an inherently non-linear feature, and that discontinuities or near-discontinuities in the response of the coating introduce strong non-linearities even with a modest acoustic drive. A specific example of this behavior is provided by the "compression only" model of Marmottant *et al.* (2005).

ACKNOWLEDGMENTS

This work is based on an invited oral presentation at the Acoustics 2012 Hong Kong Conference. The author is grateful to Dr. Michel Versluis and Dr. Jeff Ketterling for their kind invitation and to the A.S.A. for a contribution which enabled him to attend the conference. Dr. Versluis also gave generous assistance on various aspects of the project. Dr. Kausik Sarkar and Dr. Amir Katiyar kindly provided their data to facilitate the comparisons shown in Figs. 2–4. The study has been supported by NSF under grant CBET-1258398.

[1]Both contain one misprint: Sijl *et al.* (2010) omits a term in α_2 which is correctly given in Prosperetti (1977). The latter shows a factor $\omega_0^2 - \omega^2$ at the beginning of the second line of the expression for g_1 which should actually read $(\omega_0^2 - \omega^2)^{-1}$ and is correctly given in Sijl *et al.* (2010).

Brenner, M., Hilgenfeldt, S., and Lohse, D. (**2002**). "Single-bubble sonoluminescence," Rev. Mod. Phys. **74**, 425–484.
Burns, P. N., Wilson, S. R., and Simpson, D. H. (**2000**). "Pulse inversion imaging of liver blood flow: Improved method for characterizing focal masses with microbubble contrast," Invest. Radiol. **35**, 58–71.
Chomas, J., Dayton, P., May, D., and Ferrara, K. (**2002**). "Nondestructive subharmonic imaging," IEEE Trans. Ultrason. Ferroelect. Freq. Contr. **49**, 883–892.
Church, C. C. (**1995**). "The effects of an elastic solid-surface layer on the radial pulsations of gas bubbles," J. Acoust. Soc. Am. **97**, 1510–1521.
De Santis, P., Sette, D., and Wanderlingh, F. (**1967**). "Cavitation detection—The use of the subharmonic," J. Acoust. Soc. Am. **42**, 514–516.
Eller, A., and Flynn, H. G. (**1969**). "Generation of subharmonics of order one-half by bubbles in a sound field," J. Acoust. Soc. Am. **46**, 722–727.
Engquist, B., Tornberg, A.-K., and Tsai, R. (**2005**). "Discretization of Dirac delta functions in level set methods," J. Comput. Phys. **207**, 28–51.
Faez, T., Emmer, M., Docter, M., Sijl, J., Versluis, M., and de Jong, N. (**2011**). "Characterizing the subharmonic response of phospholipid-coated microbubbles for carotid imaging," Ultrasound Med. Biol. **37**, 958–970.
Frinking, P. J. A., Gaud, E., Brochot, J., and Arditi, M. (**2010**). "Subharmonic scattering of phospholipid-shell microbubbles at low acoustic pressure amplitudes," IEEE Trans. Ultrason. Ferroelect. Freq. Contr. **57**, 1762–1771.
Goertz, D. E., Frijlink, M. E., Tempel, D., Gisolf, A., Krams, R., de Jong, N., and van der Steen A. F. W. (**2007**). "Subharmonic contrast intravascular ultrasound for *vasa vasorum* imaging," Ultrasound Med. Biol. **33**, 1859–1872.
Hoff, L., Sontum, P. C., and Hovem, J. M. (**2000**). "Oscillations of polymeric microbubbles: Effect of the encapsulating shell," J. Acoust. Soc. Am. **107**, 2272–2280.
Katiyar, A., and Sarkar, K. (**2011**). "Excitation threshold for subharmonic generation from contrast microbubbles," J. Acoust. Soc. Am. **130**, 3137–3147.
Marmottant, P., van der Meer, D., Emmer, M., Versluis, M., de Jong, N., Hilgenfeldt, S., and Lohse, D. (**2005**). "A model for large-amplitude oscillations of coated bubbles accounting for buckling and rupture," J. Acoust. Soc Am. **118**, 3499–3505.
Neppiras, E. A. (**1969a**). "Subharmonic and other low-frequency emission from bubbles in sound-irradiated liquids," J. Acoust. Soc. Am. **46**, 587–601.
Neppiras, E. A. (**1969b**). "Subharmonic and other low-frequency signals from soundirradiated liquids," J. Sound Vib. **10**, 176–186.
Neppiras, E. A., and Coakley, W. T. (**1976**). "Acoustic cavitation in a focused field in water at 1 MHz," J. Sound Vib. **45**, 341–373.

Peskin, C. S. (**1977**). "Numerical analysis of blood flow in the heart," J. Comput Phys. **25**, 220–252.
Prosperetti, A. (**1974**). "Oscillations of gas bubbles in liquids: Steady-state solutions," J. Acoust. Soc. Am. **56**, 878–885.
Prosperetti, A. (**1976**). "Subharmonics and ultraharmonics in the forced oscillations of weakly nonlinear systems," Am. J. Phys. **44**, 548–554.
Prosperetti, A. (**1977**). "Application of the subharmonic threshold to the measurement of the damping of oscillating gas bubbles," J. Acoust. Soc. Am. **61**, 11–16.
Prosperetti, A. (**1991**). "The thermal behaviour of oscillating gas bubbles," J. Fluid Mech. **222**, 587–616.
Sarkar, K., Shi, W. T., Chatterjee, D., and Forsberg, F. (**2005**). "Characterization of ultrasound contrast microbubbles using *in vitro* experiments and viscous and viscoelastic interface models for encapsulation," J. Acoust. Soc. Am. **118**, 539–550.
Shankar, P. M., Krishna, P. D., and Newhouse, V. L. (**1998**). "Advantages of subharmonic over second harmonic backscatter for contrast-to-tissue echo enhancement," Ultrasound Med. Biol. **24**, 395–399.
Shankar, P. M., Krishna, P. D., and Newhouse, V. L. (**1999**). "Subharmonic backscattering from ultrasound contrast agents," J. Acoust. Soc. Am. **106**, 2101–2110.
Sijl, J., Dollet, B., Overvelde, M., Garbin, V., Rozendal, T., de Jong, N., Lohse, D., and Versluis, M. (**2010**). "Subharmonic behavior of phospholipid-coated ultrasound contrast agent microbubbles," J. Acoust. Soc. Am. **128**, 3239–3252.
Towers, J. D. (**2007**). "Two methods for discretizing a delta function supported on a level set," J. Comput. Phys. **220**, 915–931.